



OPEN

Sequence-specific inhibition of microRNA via CRISPR/CRISPRi system

SUBJECT AREAS:
EXPRESSION SYSTEMS
RNAIYicheng Zhao^{1,2*}, Zhen Dai^{2*}, Yang Liang^{1*}, Ming Yin³, Kuiying Ma³, Mei He¹, Hongsheng Ouyang² & Chun-Bo Teng¹Received
29 November 2013Accepted
13 January 2014Published
3 February 2014¹College of life science, Northeast Forestry University, Harbin, China, ²Department of Biochemistry, College of Animal Sciences, Jilin University, China, ³College of Veterinary Medicine, Jilin University, China.

Here, we report a convenient and efficient miRNA inhibition strategy employing the CRISPR system. Using specifically designed gRNAs, miRNA gene has been cut at a single site by Cas9, resulting in knockdown of the miRNA in murine cells. Using a modified CRISPR interference system (CRISPRi), inactive Cas9 can reversibly prevent the expression of both monocistronic miRNAs and polycistronic miRNA clusters. Furthermore, CRISPR/CRISPRi is also capable of suppressing genes in porcine cells.

Correspondence and requests for materials should be addressed to C.-B.T. (chunboteng@nefu.edu.cn) or H.O. (oyhs64@hotmail.com)

* These authors contributed equally to this work.

MicroRNAs (miRNAs), a class of highly conserved non-coding regulatory factors, are present throughout the eukaryotic genome and are predicted to negatively regulate more than half of the protein-coding genes in mammals¹. miRNAs are essential to most biological processes, including proliferation, differentiation and apoptosis, and their transcription is tightly controlled¹. Aberrant miRNA expression has been associated with numerous diseases. For instance, leukemia involves increased production of *miR-17-92* cluster miRNAs, whereas glioblastoma is linked to elevated amounts of *miR-21*^{2,3}. miRNA inhibition is used to elucidate miRNA function and to treat diseases related to these functions. Currently, chemically modified complementary antisense oligonucleotides (ASOs) are widely used as miRNA silencers *in vitro*; however, ASOs typically require expensive modifications and usually generate off-target effects⁴. In addition, the generation of loss-of-function miRNA mutations via homologous recombination is technically difficult because the transcripts are usually short⁵. Therefore, a precise and efficient miRNA inhibition technology would prove useful.

Recent advances in the study of the prokaryotic CRISPR adaptive immune system allow for an alternative genome editing approach^{6,7}. Using a specifically designed crRNA-tracrRNA duplex, termed gRNA, Cas9 can be directed to the sequence of interest, generating DNA double-strand breaks (DSBs) that result in gene silencing. Such easily engineered systems are increasingly being employed and have been successful to knock out protein-coding genes in several model organisms. To our knowledge, only one study has reported the silencing of non-coding miRNA genes using CRISPR⁸. However, the success achieved in that case required simultaneous generation of two DSBs in the genome, and it remains unknown whether a single cut event is capable of affecting miRNA gene expression.

Results and discussion

It is well known that the pre-mature of miRNA exist as a classical stem-loop structure. Theoretically, DSBs in the loop region could affect miRNA maturation during processing by Droscha and Dicer. To test this hypothesis, three exogenous short hairpin RNAs (shRNA1-3, Table. S1) were employed as substitute miRNAs because of their similar stem-loop morphology⁹. Based on the Massively Parallel Sensor Assay¹⁰, we established three stable NIH3T3 reporter cell lines, each of which expressed a doxycycline-inducible shRNA and a Venus-sensor fusion protein containing the target shRNA region (Fig. 1 A) to enhance measurement sensitivity. The fluorescence intensity was detected using flow cytometry analysis (FCM) and represented the total amount of viable shRNA (Fig. 1 A). crRNAs were designed to separately recognize the linker between the loop and seed region of shRNA1-3 in the three vectors (Crispsh1-3) (Fig. 1 B). After transient transfection of Crispsh1, 2 and 3 separately into the corresponding reporter cell lines, a significant enhancement of fluorescence signal was detected (Fig. 1 C-D), indicating that the inhibition of the targeted shRNAs might result from specific DSBs in the target regions.

To confirm the specificity and efficiency of DNA cutting, the targeted region in each shRNA was amplified from DNA extracted from the reporter cell strain. The purified PCR products were denatured and reannealed to form hybridized DNA and then treated with the Transgenomic SURVEYOR[®] Mutation Detection Kit, which recognizes and cleaves mismatched DNA. As shown in Fig. S1 A, control shRNA yielded two bands (with a

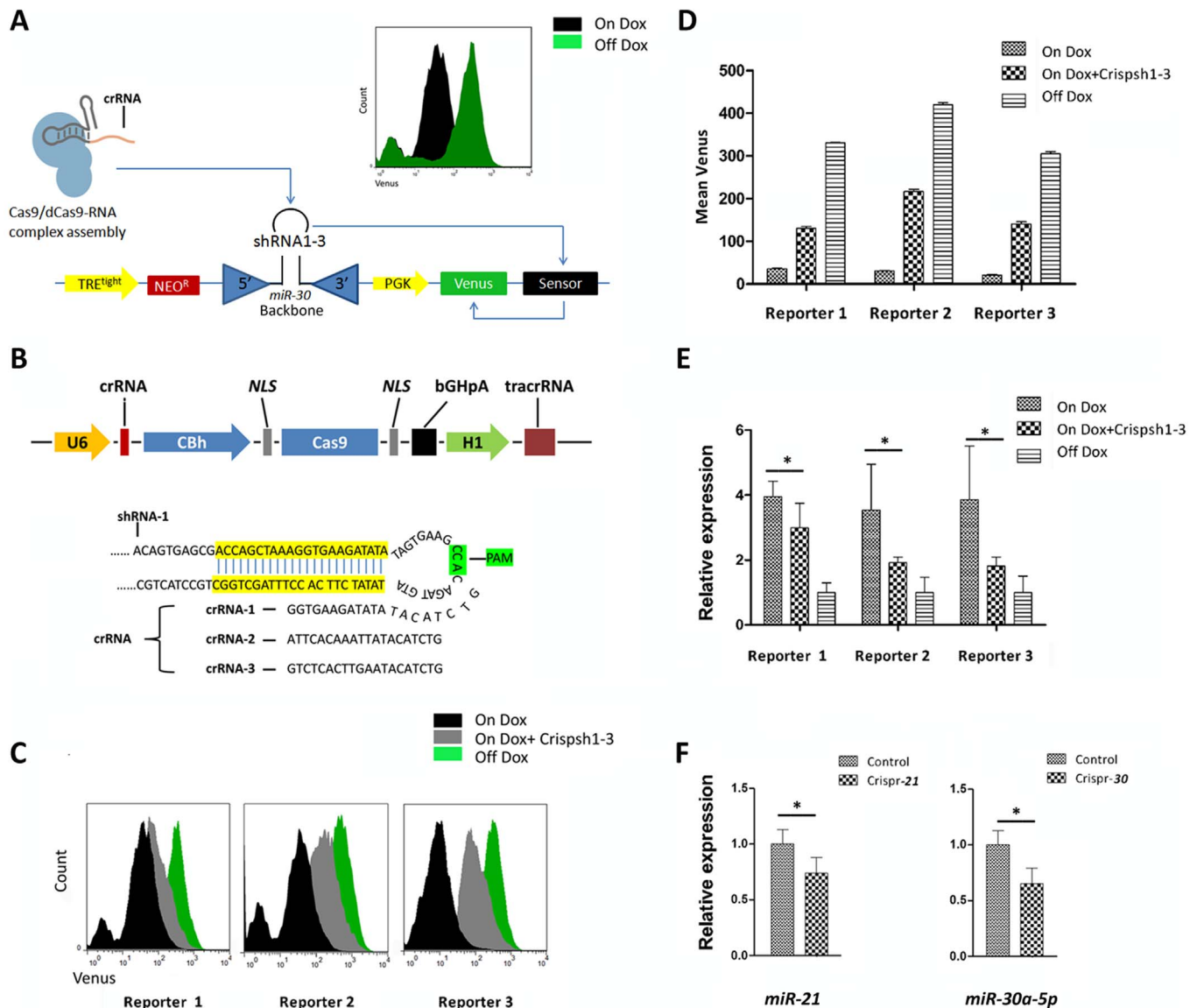


Figure 1 | Inhibition of exogenous shRNAs and miRNAs via CRISPR. (A). The reporter vector encodes a Tet-inducible shRNA and its cognate target sequence downstream of a PGK-driven Venus reporter. Upon infection of cells expressing rtTA, Dox treatment induces shRNA expression, which is repressed by the Cas9-RNA complex. In turn, the difference in Venus expression indirectly suggests CRISPR/CRISPRi potency. Histograms of flow cytometry results depicting the fluorescence intensity distributions for the shRNAs after adding Dox. The leftmost peaks represent uninfected cells. (B). The CRISPR system consists of a single protein, Cas9, and two designed RNA elements forming a duplex (gRNA). Cas9 is guided by the gRNA to cleave the target site at -20 nt. PAM, an NGG motif shown in green, is essential for the activity of the complex. The crRNA contains approximately 20 nt of unique target spacer sequence; here, all their three sequences were designed to be complementary to the linker of the loop and seed region of the shRNAs. (C). Three shRNA-venus reporter cells were transfected with repressing vectors (Crispsh1, Crispsh2 or Crispsh3) encoding the Cas9/gRNA cassettes and were assayed with or without Dox (On/Off Dox). Fluorescence intensity distribution after 72 h indicated significant repression of shRNAs by CRISPR. (D). Relative fluorescence intensity is shown in the diagrams. The inhibition effect of CRISPR was 40–50% for each shRNA. The values shown are the means of three replicates. (E). Correlation of the reads per shRNA displays a strong repressive effect on miRNAs (20–50% fold) as assayed using quantitative PCR. The values are the means of three replicates. (F). NIH3T3 cells were transfected with Crisp-21 and Crisp-30. The qPCR data show that transfection of each vector can repress endogenous *miR-21* and *miR-30a* miRNA expression. The values shown are the means of three replicates, and each miRNA was normalized to an internal control, U6 RNA. Single star indicated $P < 0.05$.

weaker signal from the smaller band) when resolved using gel electrophoresis because its native palindromic sequence can form a loop (which causes mispairing during reannealing). However, each targeted shRNA produced two bands with a brighter low band than the control, indicating that the mispairing mutations in the amplicon of the targeted region (Fig. S1 A) resulted from the cleavage of Cas9.

Interestingly, DNA sequencing analysis of the shRNA3 amplicons was inconsistent with previous reports¹⁵; the Cas9 locus in our data was distant from the anticipated site, which may have been caused by the

self-forming loop structure of DNA (Fig. S1 B). Our results demonstrated that Cas9/gRNA could specifically cleave an shRNA expression cassette in NIH3T3 cells. Such damage might result in DSB in shRNA transcripts; however, it was not determined directly whether DSBs could repress miRNA maturation. Quantitative PCR (qPCR) analysis was then performed to detect all three mature shRNAs in the reporter cell lines, and the results confirmed a strong repressive effect (30–50%) (Fig. 1 E). Our data also demonstrated that Cas9 could target the special loop region adjacent to the palindromic sequence.

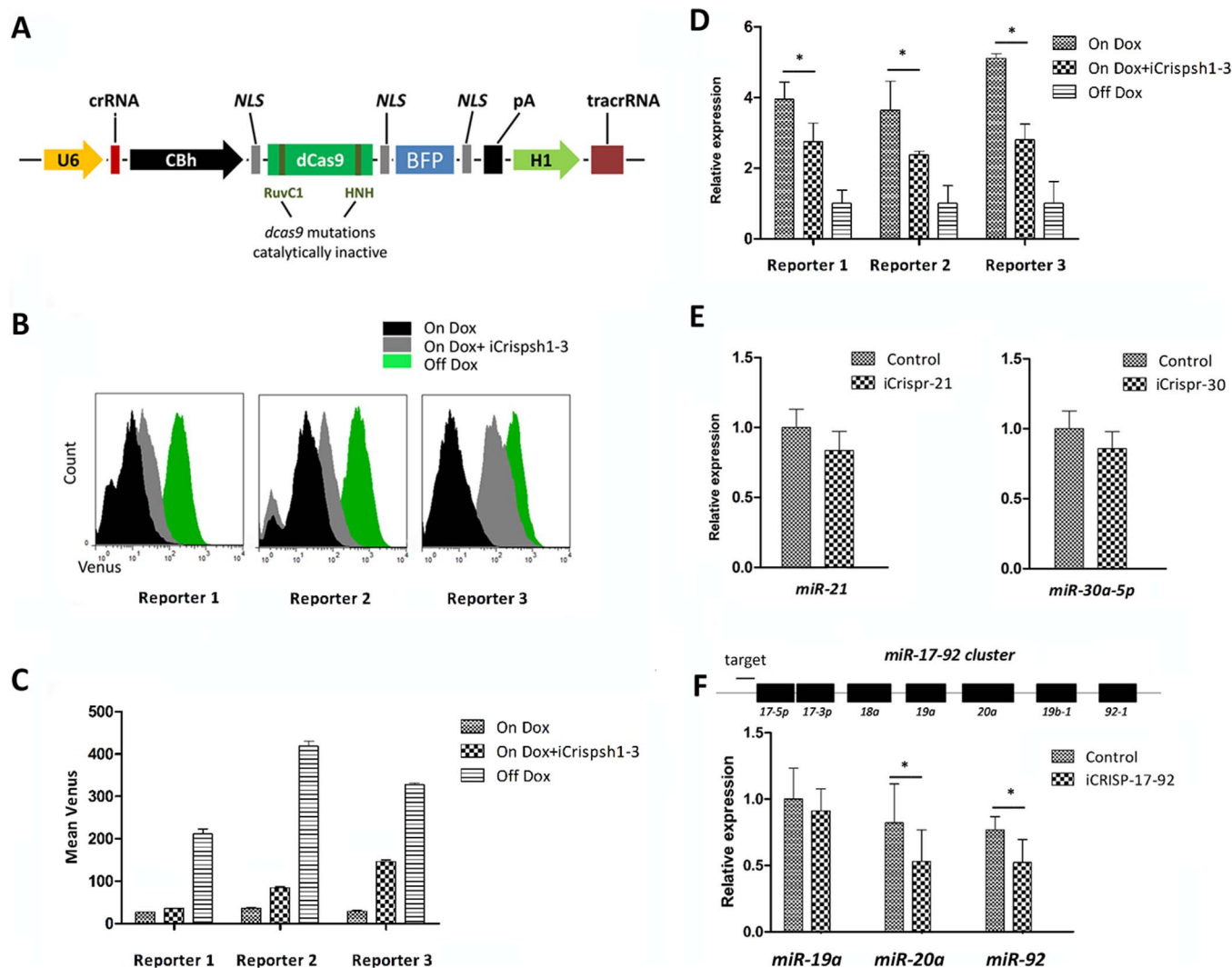


Figure 2 | Repression of shRNAs and miRNAs using CRISPRi in NIH3T3 cells. (A). The CRISPRi system consists of a fusion protein and two designable RNA elements. The dCas9 protein is defective for nuclease activity but can block RNA polymerase binding and transcriptional elongation when targeting occurs. All crRNA sequences were identical to those described in Table S1. (B). FCM of reporter cells transfected with iCrisps1, iCrisps2 or iCrisps3 carrying dCas9/gRNA cassettes, with or without Dox treatment (On/Off Dox). The fluorescence intensity distribution after 72 h indicated significant repression of the shRNAs by CRISPRi. (C). Relative analysis histograms were generated from FCM. The inhibition effect of CRISPRi was 40–50% for each shRNA. The values shown are the means of three replicates. (D). Examination of the reads per shRNA indicated a strong repressive effect on miRNAs (10–30% fold) as assayed using quantitative PCR. The values shown are the means of three replicates. (E). NIH3T3 cells were transfected with iCrispr-21 and iCrispr-30. The qPCR data show that transfection of repressing vector can inhibit endogenous *miR-21* and *miR-30a* miRNA expression. The values shown are the means of three replicates, and each miRNA was normalized to an internal control, U6 RNA. (F). The *miR-17-92* cluster encodes 7 miRNAs. A crRNA targeting an area upstream of the cluster was designed for use with CRISPRi. We hypothesized that iCrispr-17-92 was able to repress all miRNA expression within the entire cluster by transcriptional elongation blockage. qPCR was performed in three replicates, there was a repressive effect on *miR-19a* expression (10% fold) and significant repression of *miR-20a* and *miR-92-1* expression was observed (20–25% fold). The values shown are the means of three replicates. Single star indicated $P < 0.05$.

To investigate whether CRISPR can knock out endogenous miRNAs, two representative monocistronic miRNAs were chosen. The first was *miR-21*, an oncomiR that is highly expressed in 3T3 cells, and the second was *miR-30a*, which contains the same looped backbone as the previously tested shRNAs. After transfection with the corresponding repressing vector (Table S2), both miRNAs were efficiently silenced (Fig. 1 F). These results demonstrated that miRNA expression can be suppressed in murine cells by cutting the genome at a single site with Cas9.

An earlier article reported a reversible approach to selectively control gene expression on a genome-wide scale via a modified CRISPR interference system (CRISPRi). Targeting of catalytically inactive Cas9 protein (dCas9) to the coding region of a gene can

sterically block binding or elongation of RNA polymerase and leads to disruption of gene transcription in bacteria and human cells¹². Because Cas9/gRNA can efficiently target a specific region of shRNA, dCas9/gRNA might possess similar recognition ability. To obtain deeper insight into this point, we cloned crRNAs into vectors (iCrisps1, 2 and 3) expressing catalytically inactive dCas9 with mutations in the RuvC1 and HNH nuclease domains (Fig. 2 A). The resulting transfection results showed that shRNA expression was also inhibited by this non-nuclease method (Fig. 2 B–D), as were the expression levels of *miR-21* and *miR-30a* when each repressing vector was transfected into NIH3T3 cells (Fig. 2 E). A decrease in the repressive ability of CRISPRi was observed compared to CRISPR, possibly due to enzymatic inactivation.

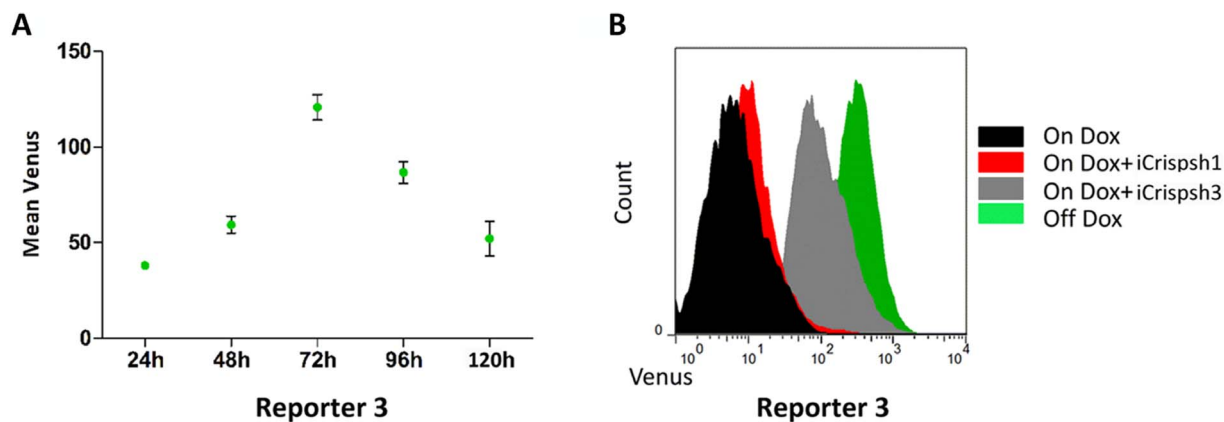


Figure 3 | CRISPRi regulation is reversible and specific. (A). Actual sorts of cells using Venus/FSC dot plots. The reporter 3 cell line treated with Dox and iCrispsh3 was assessed at different times. The fluorescence signal started to increase at 24 h and took approximately 72 h to reach a peak, after which the signal decayed. The values shown are the means of three replicates. (B). Data are presented as fluorescence intensity histograms. Addition of iCrispsh1 to the shRNA3 reporter cell line did not enhance the fluorescence signal.

One advantage over knockout methods is that CRISPRi-based knockdown might be reversible¹². To confirm this effect reported by Qi et al.¹², we analyzed the fluorescence intensity in the shRNA3 reporter cell line at different times and found that the signal reached a maximum level at 72 h and then decreased to the control level after a further 48 h (Fig. 3 A). In addition, transfection of iCrispsh1 into the shRNA3 reporter cell line revealed no off-target effects from CRISPRi (Fig. 3 B).

Furthermore, blockage of the upstream region of miRNA clusters is thought to affect all downstream miRNAs. To test this hypothesis, CRISPRi targeting the *miR-17-92* cluster was performed in mouse bone marrow stem cells (BMSCs). The crRNA used was designed to localize to the upstream region of *miR-17* (Fig. 2 F). When nucleotide sequences of the members of the *miR-17-92* cluster were aligned, they could be roughly divided into three groups (*miR-20a*, *miR-17* and *miR-18a*; *miR-19a* and *miR-19b-1*; *miR-92-1*). To assess the knock-down efficiency of CRISPRi, the expression of mature *miR-19a*, *miR-20a* and *miR-92-1*¹³ were detected. As measured using qPCR, all three miRNAs were repressed 48 h after transfection with the single vector iCrisp-17-92 (Fig. 2 F). These data demonstrate that it is feasible to disrupt endogenous monocistronic and cluster mouse miRNAs via CRISPRi.

Our research interest focuses on the regulatory function of miRNAs in mammalian development and human disease^{14,15}. Recently, it was reported that the failure of some mouse models to replicate human pathology was due to the biological differences between the two species. In fact, pigs are more physiologically similar to humans than rodents and other laboratory animals¹⁶. One group has reported CRISPR/Cas9-mediated homology-directed repair (HDRs) in pigs; however, a lower cell recovery rate using the CRISPR strategy was observed¹⁷. To test whether CRISPR/CRISPRi could efficiently repress gene expression in pigs, we carried out a similar *EGFP* experiment according to the method of Qi and Zhang et al.^{12,18} in porcine cells.

We constructed four vectors (designated as Crispgfp1, 2 and iCrispgfp1, 2) targeted to two sites of *EGFP* (Fig. S2 A). After transfecting Crispgfp1/2 and iCrispgfp1/2 vectors separately into clonal *EGFP*-positive PK-15 cells, FCM analysis showed significant differences between the Cas9/dCas9 cells and control cells (Fig. S2 B). To locate the cleavage site precisely, we sequenced the amplified *EGFP* products from Crispgfp2-transfected cells and found three mutant clones out of the 40 sequenced. The cleavage occurred 5 nt away from the protospacer adjacent motif (PAM) required for Cas9 targeting (Fig. S2 C). These results demonstrate that CRISPR/CRISPRi can site-specifically disrupt gene expression in porcine cells. To enhance the sensitivity, PK-15 cells were first infected with

retroviruses containing inducible shRNA3 and the Venus-sensor components. Then, the vectors Crispsh3 and iCrispsh3 were transfected into shRNA3-positive PK-15 cells, and the divisional changes in fluorescence compared to the control were detected by FCM. A qPCR assay also showed decreased expression of mature shRNAs after transfection (Fig. S3 A–C).

All of our results indicate that CRISPRi can also be used to inhibit miRNA expression in pigs. In earlier reports, the persistence and efficiency of CRISPR or TALEs had a dosage-dependent effect when knocking out genes^{19,20}. However, increasing the dosage of dCas9/gRNA was not able to improve the efficiency but instead led to severe toxicity in our experiments (data not shown). In addition, a modest cut/block efficiency was observed in PK-15 cells compared to NIH3T3 cells. The toxicity may result from target-off effects by Cas9 or IFN effects by gRNAs^{21,22}, the low efficiency may be committed by lack of optimal codon or insufficient NLS (nuclear localization signals)^{20,23}. Therefore, improvement of this method for researchers interested in controlling porcine gene expression will be required in the future.

In summary, the CRISPR/CRISPRi system can be easily adapted to target a miRNA sequence by simply switching the crRNA in a single repression vector, which entails changing only a 20-bp sequence. This makes CRISPR/CRISPRi more convenient to engineer, particularly if one desires to generate vectors that target multiple miRNAs. Another potential advantage of the CRISPRi system is that a single vector can repress multiple targets within a miRNA cluster with reduced toxicity. Our results have demonstrated that the system can specifically silence miRNAs in mice and swine with no detectable off-target effects. Compared with other strategies, the CRISPR/CRISPRi system is easier to engineer and exhibits improved flexibility as a tool to analyze miRNA function and for future disease therapy.

Methods

Ethics statement. All animal experiments were conducted according to the guidelines for animal care and use established by the Northeast Forestry University Animal Care and Use Committee.

Plasmid design and construction. The vector MSCV-tre-neo-mirna-pgk-Venus-sensor and vector MSCV-rTA3-PGK-Puro were constructed based on the tMSCV retroviral backbone (Clontech) using standard cloning techniques. The sensor vector included an improved Tet-responsive element promoter (TRE^{igbt}, cloned from TrMPVIR, <http://www.addgene.org/27995/>), a neomycin resistance (Neo^R) marker harboring the human *miR-30* scaffold in its 3' UTR (cloned from pPRIME-CMV-Neo, <http://www.addgene.org/11665/>) and a PGK promoter driving the expression of Venus (cloned from TrMPVIR). The plasmids (Crispsh 1–3) were constructed using a px260 backbone (<http://www.addgene.org/42229/>). The dCas9-BFP fusion CDS containing a humanized dCas9 gene was cloned from vector pdCas9-humanized



(<http://www.addgene.org/44246/>). Detailed vector maps, sequence information and cloning protocols are available on request.

Cell culture and DNA transfection. Mouse BMSCs were obtained from tibia and fibula bone marrow as described by M. Soleimani et al.²⁴. NIH3T3 and PK-15 cell lines were cultured in Dulbecco's modified Eagle's medium containing 10% fetal bovine serum under humidified conditions in 95% air and 5% CO₂ at 37°C. DNA transfection was performed using Lipofectamine® LTX Reagent (Invitrogen). Primer sequences are listed in Table S1.

Establishment of shRNA1-3 reporter clonal cell lines. The packaging cell line 293GP was transfected with 5 µg plasmid DNA and 5 µg helper plasmid using Lipofectamine 2000 (Invitrogen). NIH3T3-Sh1-3 clonal reporter cells were generated by co-infection of NIH3T3 cells with two vsv-g pseudotyped retroviruses, MSCV-rRTA3-PGK-Puro and MSCV-tre-neo-mirna-pgk-Venus-sensor. Retroviral co-transduction was performed with fluorescent reporter constructs, and the cells were assessed 48 h post-infection using FCM (BD). Transduced cell populations were usually selected 48 h after infection using 2.0–2.5 µg/ml puromycin (Sigma-Aldrich) or 1,000 µg/ml G418 (Amresco) for 3T3 cells. PK-15 EGFP-positive clonal cells were generated from MSCV-cmv-egfp-pgk-puro using 1,500 µg/ml puromycin²⁵. Tet-regulated shRNAs were induced using Dox concentrations (Sigma-Aldrich) of 1.0–2.0 µg/ml in 3T3 cells and 2.0–4.0 mg/ml in PK-15 cells.

Flow cytometry and analysis. All FCM procedures were performed using a FACScan (BD) instrument. The cells were trypsinized and centrifuged at 300 × g for 5 min 24–120 h post-transfection. The resulting pellet was washed with cold wash buffer and resuspended at a density of 10⁵ cells/ml. After a second wash, the cells were analyzed using FACScan flow cytometry. The data were analyzed using Flowjo. For each experiment, triplicate cultures were measured.

MicroRNA extraction and qPCR amplification. miRNAs were purified using an miRcute microRNA isolation kit (TIANGEN). Polyadenylation was performed using 5 U of poly(A) polymerase (NEB). Reverse transcription was performed using an miRcute miRNA first-strand cDNA kit (TIANGEN). All transcripts were assayed in three replicates using the iQ™ 5 Multicolor Real-time PCR Detection System (Bio-Rad) and an miRcute miRNA qPCR detection kit. All results were normalized to the U6 small nuclear RNA. Relative amounts of RNA transcripts were analyzed using the standard curve method, and the error bars indicate the standard deviation. All of the primers used in our research are listed in Supplementary Table S2.

1. Svoboda, P. & Stein, P. RNAi experiments in mouse oocytes and early embryos. *Cold Spring Harb Protoc* **2009**, pdb top56 (2009).
2. Kilic, T. et al. Electrochemical based detection of microRNA, mir21 in breast cancer cells. *Biosens Bioelectron* **38**, 195–201 (2012).
3. Patel, V. et al. miR-17 ~ 92 miRNA cluster promotes kidney cyst growth in polycystic kidney disease. *Proc Natl Acad Sci U S A* **110**, 10765–70 (2013).
4. Lanford, R. E. et al. Therapeutic silencing of microRNA-122 in primates with chronic hepatitis C virus infection. *Science* **327**, 198–201 (2010).
5. Gentner, B. et al. Stable knockdown of microRNA in vivo by lentiviral vectors. *Nat Methods* **6**, 63–6 (2009).
6. Wiedenheft, B. In defense of phage: Viral suppressors of CRISPR-mediated adaptive immunity in bacteria. *RNA Biol* **10** (2013).
7. Elmore, J. R. et al. Programmable plasmid interference by the CRISPR-Cas system in *Thermococcus kodakarensis*. *RNA Biol* **10**, 828–40 (2013).
8. Xiao, A. et al. Chromosomal deletions and inversions mediated by TALENs and CRISPR/Cas in zebrafish. *Nucleic Acids Res* **41**, e141 (2013).
9. Brummelkamp, T. R., Bernards, R. & Agami, R. A system for stable expression of short interfering RNAs in mammalian cells. *Science* **296**, 550–3 (2002).
10. Fellmann, C. et al. Functional identification of optimized RNAi triggers using a massively parallel sensor assay. *Mol Cell* **41**, 733–46 (2011).

11. Shen, B. et al. Generation of gene-modified mice via Cas9/RNA-mediated gene targeting. *Cell Res* **23**, 720–3 (2013).
12. Qi, L. S. et al. Repurposing CRISPR as an RNA-guided platform for sequence-specific control of gene expression. *Cell* **152**, 1173–83 (2013).
13. Kanzaki, H. et al. Identification of direct targets for the miR-17-92 cluster by proteomic analysis. *Proteomics* **11**, 3531–9 (2011).
14. Yang, Y. et al. MiR-18a regulates expression of the pancreatic transcription factor Ptf1a in pancreatic progenitor and acinar cells. *FEBS Lett* **586**, 422–7 (2012).
15. Zhang, Z. W. et al. MicroRNA-19b downregulates insulin 1 through targeting transcription factor NeuroD1. *FEBS Lett* **585**, 2592–8 (2011).
16. Yang, D. et al. Expression of Huntington's disease protein results in apoptotic neurons in the brains of cloned transgenic pigs. *Hum Mol Genet* **19**, 3983–94 (2010).
17. Tan, W. et al. Efficient nonmeiotic allele introgression in livestock using custom endonucleases. *Proc Natl Acad Sci U S A* (2013).
18. Shen, B. et al. Generation of gene-modified mice via Cas9/RNA-mediated gene targeting. *Cell Res* (2013).
19. Joung, J. K. & Sander, J. D. TALENs: a widely applicable technology for targeted genome editing. *Nat Rev Mol Cell Biol* **14**, 49–55 (2013).
20. Gilbert, L. A. et al. CRISPR-Mediated Modular RNA-Guided Regulation of Transcription in Eukaryotes. *Cell* **154**, 442–51 (2013).
21. Ran, F. A. et al. Double nicking by RNA-guided CRISPR Cas9 for enhanced genome editing specificity. *Cell* **154**, 1380–9 (2013).
22. Olejniczak, M., Galka-Marciniak, P., Polak, K., Fligier, A. & Krzyzosiak, W. J. RNAimmuno: a database of the nonspecific immunological effects of RNA interference and microRNA reagents. *RNA* **18**, 930–5 (2012).
23. Mashiko, D. et al. Generation of mutant mice by pronuclear injection of circular plasmid expressing Cas9 and single guided RNA. *Sci Rep* **3**, 3355 (2013).
24. Soleimani, M. & Nadri, S. A protocol for isolation and culture of mesenchymal stem cells from mouse bone marrow. *Nat Protoc* **4**, 102–6 (2009).
25. Zhao, Y. et al. Human MxA protein inhibits the replication of classical swine fever virus. *Virus Res* **156**, 151–5 (2011).

Acknowledgments

This work was supported by the Fundamental Research Funds for the Central Universities (No. DL13BAX03) and the National Natural Science Foundation of China (No. 31272520). We thank Dr. Feng Yang (Department of Molecular Endocrinology, San Diego School of Medicine, University of California, USA) and Prof. Hongkui Deng (College of Life Sciences and Peking-Tsinghua Center for Life Sciences, Peking University) for significant advice and technical support.

Author contributions

Y.C.Z., Z.D. & M.H. wrote the main manuscript text, K.Y.M. and M.Y. prepared figure S1 & S2. Y.C.Z., Z.D. & Y.L. prepared Fig. 1, Fig. 2, Fig. 3 and Fig. S3. C.B.T., H.S.O.Y. and all the other authors have reviewed the manuscript.

Additional information

Supplementary information accompanies this paper at <http://www.nature.com/scientificreports>

Competing financial interests: The authors declare no competing financial interests.

How to cite this article: Zhao, Y.C. et al. Sequence-specific inhibition of microRNA via CRISPR/CRISPRi system. *Sci. Rep.* **4**, 3943; DOI:10.1038/srep03943 (2014).



This work is licensed under a Creative Commons Attribution-NonCommercial-NoDerivs 3.0 Unported license. To view a copy of this license, visit <http://creativecommons.org/licenses/by-nc-nd/3.0>